International Journal of Geography and Geology
2013 Vol. 2, No. 2, pp. 14-23
ISSN(e): 2305-7041
ISSN(p): 2306-9872
DOI: 10.18488/journal.10/2013.2.2/10.2.14.23

A STUDY OF STREAM SEDIMENTS FROM SOLTAN MEYDAN BASALTIC FORMATION AREA, NORTHERN IRAN

Mehdi Hashemi Gahruei[1] --- Majid Gholami[2] --- Teimoor Nazari Dehkordi[3]†

[1,2]*Department of Geology, Faculty of Sciences, Golestan University, Gorgan, Iran*

[3]*Department of Earth Sciences, Faculty of Sciences, Shiraz University, Shiraz, Iran*

ABSTRACT

Stream sediments of the Eastern Alborz Mountain located at Northern Iran, were studied at Silurian-formed Soltan Meydan Basaltic Formation area. The area which is mainly consisted of basalt, andesite and tuff represents a structurally active zone, with Mountain Front Sinuosity index (S_{mf}) of 1.2, caused development of numerous faults, prominently with NE-SW trend. Assessment of potential for metallic mineral deposits in the area was carried out using stream sediment sampling and remote sensing. Total metal concentration in the AAS-analyzed sediments varies in the range of Cu: 33-106.54 ppm, Pb: 14.46-189.04 ppm, Zn: 40.88-376 ppm, Ni: 15.14-73.24 ppm, Co: 8.2-88.64 ppm, Mn: 321.6-1326.4 ppm, and Fe: 2.28-5.39 wt%. Statistical processing of geochemical data shows two concentrated areas as geochemical anomalies. These areas are matched with those which are presented by Photo-lineament Factor (PF) indicating high density of regional structures and tectonic features. Taking high-concentrated-fractured areas into account, it is suggested that there is a close relationship between structural features and the possibility of mineralization which explains that the stream sediments could have been enriched by streams flowing through well-developed drainage system.

Keywords: Stream sediments, Photo-lineament factor (PF), Geochemical anomaly, Soltan meydan basaltic formation, Iran

Received: 1 April 2013/ **Revised:** 3 May 2013/ **Accepted:** 8 May 2013/ **Published:** 13 May 2013

INTRODUCTION

Mineral deposits represent anomalous concentrations of specific elements, of which usually include a central zone, or core, often in percentage quantities, to a degree sufficient to permit economic exploitation. Although the elements surrounding this zone generally decrease in

† Corresponding author

concentration until they reach levels, which appreciably exceed the normal background level of the enclosing rocks, in some cases mineral deposits either on or near the surface, are subject to both chemical and physical factors of weathering. Many of the ore minerals undergo decomposition or disintegration and their chemical constituents become dispersed into weathering debris, soils, ground water, and plant tissue. Further dispersion, often over considerable distances, may ensue due to the agencies of glaciers or stream systems (Dugmore *et al*., 1996; Le Couteur and Mcleod, 2006; Sarala and Peuraniemi, 2007; Champan *et al*., 2009).

Geochemical surveys based on analyzing of stream sediments are a well studied technique to find anomalous concentrations of specific elements that, over five decades, has been used worldwide wherever stream drainage systems are well established. This usage is based on the cost-effective ability of such surveys to identify anomalous watersheds as targets for further exploration and to give economic guidelines that may help interpret the autogenic and non-autogenic geochemical anomalies (Bull, 1997; Duk-Rodkin *et al*., 2003; Ohta *et al*., 2004; Atsuyuki *et al*., 2005). To extract topographic information and modeling of surface processes a Digital Elevation Model (DEM) has been offered. DEMs can be generated from contour lines, with radar-interferometry data derived, most importantly, from Space Shuttle Radar Topography Mapping mission (SRTM) (Duncan, 1998; Bishop, 2001; Paul *et al*., 2004; Seleem, 2013).

The purpose of this study is to investigate the stream sediments of Soltan Meydan Basaltic Formation area by analyzing selected samples to indicate anomalous concentrations of copper, lead, zinc, iron, nickel, cobalt and manganese, which has been followed by applying SRTM DEM satellite images to evaluate the relationship between the remote sensing-derived aligned features, Photo-lineament Factor (PF), and the possibility of finding mineral potential areas.

Geological Setting

Paleozoic-Mesozoic rocks crop out extensively and with great thickness in the Eastern Alborz Mountain of Northern Iran consist of, in ascending stratigraphic order, the Abarsaj (arkosic sandstone with muscovite, Ordovician), Soltan Meydan (basalt-andesite-tuff, Silurian), Padeha (quartz-arenite sandstone, Upper Devonian), Khosh-Yeylagh (dolomite-limestone-sandstone and conglomerate, Upper Devonian), Mobarak (limestone and shale, Lower Carboniferous), Dorud (sandstone and shale, Permian), Elika (dolomite and sandstone, Triassic) and Shemshak (sandstone and shale, Jurassic) Formations (Ghavidel-Syooki, 2000; Ghavidel-Syooki and Vecoli, 2007).

Soltan Meydan Basaltic Formation is situated at the southern edge of Eastern Alborz Mountains, Semnan Province, in Northern Iran and includes sporadic magmatic body exposure. The main fault zone with NE-SW trend which reaches to Shahrud City represents a structurally active zone caused development of numerous faults and conforms to the regional fault zone, named Northern Shahrud Fault Zone (Fig. 1). This area was formed in an extensional intra-continental setting and signifies the early stages of opening and formation of Paleo-Tethys in Silurian. The Ordovician period was coincided with the beginning of extension, Alborz separation and Paleo-Tethys formation which was accompanied by emplacement of magmatic bodies until Devonian. The evidence suggests that Iranian platform was subjected to uplift, continental crust extension and rifting during Ordovician to Devonian (Berberian, 1983; Alavi, 1996). Prior to the Ordovician time, the extension was accompanied by formation of normal faults showing turbiditic facies in a shallow sea environment. The thick mass of extrusive and intrusive igneous rocks (with an approximate thickness of 1000 meters) with an age of Middle Ordovician to Devonian described in Alborz Mountains indicates an obviously mafic composition. The volcanic rocks of the complex include pyroclastic and volcano clastic rocks with interpretations of andesitic and basaltic lava flows consist Soltan Meydan Basaltic Formation exposing at Abr, Abarsaj and Mighan villages at the NE of Shahrud City and is emplaced at the basal part of Khosh-Yeylagh Formation (Mehdizadeh, 2008) (Fig. 1).

Satellite Image Processing

To identify regional structures and to prepare a map of streams from the study area SRTM DEM images with a resolution of 45 meters have been employed. These images have an advantage of the possibility of setting up the position of scene illumination, thus emphasizing the different existing structural orientations due to the enhancement of directions perpendicular to lighting in spite of parallel ones (Masoud and Koike, 2006; Solomon and Ghebreab, 2006) (Fig. 2).

To evaluate the intensity of tectonic activity, the following formula has been applied dubbed Mountain Front Sinuosity index (Bull and McFadden, 1977):

(Equation 1) $$S_{mf}= L_{mf}/L_s$$

In the equation 1;

L_{mf}) the length of mountain front or flank's curve and L_s) the length of mountain front or flank's straight line.

To study the lineaments, a multiple of filters can be applied on satellite images with the result of revealing density and orientation more efficiently (Honarmand and Ranjbar, 2004). Most often, the lineaments cannot be discerned on satellite images straightforward but some are more easily explained as a result of the suitable conditions of lighting on the ground including absence/presence of vegetation and orientation of streams (Hardcastle, 1995). In order to get a higher resolution image and depict the features better, a combination of visible bounds (VNIR) with a 2-3(N)-1 sequence and 3(B) band was used to help obtain a resolution of 15 meters. Afterwards, by applying various geomorphologic and oriented filters at different angels (45, 90 and 135) with a core of 3*3, the feature variances with the widest range and most suitable values were chosen and depicted. At the next stage, the Photo-lineament Factor (PF) was calculated by extracting the layer of features. This factor is a well established method for calculating lineament index of satellite images and aerial photographs (Singh, 2003; Honarmand and Ranjbar, 2004). Hence, the following equation is the foundation of the method used (Fig. 3):

(Equation 2) $PF= (a/A) + (b/B) + (c/C) + (d/D)$

In the equation 2;

a) the number of lineaments available in each cell, A) their average on the map, b) the length of lineaments in each cell, B) their average on the map, c) the number of intersections of lineament per cell, C) their average on the map, d) the number of lineament groups in each cell, and D) their average on the map. Based on these parameters a grid whit appropriate cell dimension of 1*1 kilometers for the study area has been designed and deployed on the map of lineaments calculated each parameter, in turn, for each cell in order to analyzing the lineaments.

Sampling and Analyzing Process

The geochemical samples, 62 in number, were collected with a frequency of one sample per square kilometer from designated points on the maps of Abarsaj and Qaleh-Nowkhareqan villages of a scale of 1:50000, showing on the figure 4, from a depth of 20 to 30 centimeters at the middle or near the edge of active streams. It is noteworthy that all sample locations were far from contaminant sources such as rural and industrial areas and were mainly fresh and representative. The samples were placed in safe bags and transported to the laboratory. The hand trowel was washed with a detergent, rinsed and dried before each use so as to minimize contamination. Sediment samples were air dried and 300 g were transferred into a set of standard sieves (0.063 mm, 0.125 mm, 0.25 mm, 0.5 mm, 1.0 mm and 2.0 mm) with the largest mesh size on top and the smallest at the bottom. The sieving was carried out using a vibrating machine.

The total content of copper, lead, zinc, cobalt, manganese, iron and nickel in sediment fractions was determined using the method as described by Sekabira *et al.* (2010). Ideally, 1.25 g of each sample was digested with 20 mL aqua regia (HCl/HNO_3; 3:1) in a beaker (open-beaker digestion) on a thermostatically controlled hot plate. The digest was heated to near dryness and cooled to ambient temperature. Then 5.0 mL of hydrogen peroxide was added in parts to complete the digestion and the resulting mixture heated again to near dryness in a fume cupboard. The beaker wall was washed with 10 ml of de-ionized water and 5.0 ml HCl were added, mixed and heated again. The resulting digest was allowed to cool and transferred into a 50 mL standard flask and made up to the mark with de-ionized water. Copper, lead, zinc, cobalt, manganese, iron and nickel were then analyzed by direct aspiration of the sample solution into a Perkin-Elmer model 2380 Flame Atomic Absorption Spectrophotometer (AAS). All metals were analyzed using lean-blue acetylene flame at wavelength 324.8 nm, slit width 0.2 mm and sensitivity check of 5.0 mg/L Cu; wavelength 228.8 nm, slit width 0.7 and sensitivity check of 2.0 mg/L Cd; wavelength 213.9 nm, slit size 0.7 nm and sensitivity check 9.0 mg/L Pb and wavelength 279.5 nm, slit size 0.2 nm and sensitivity check of 2.5 mg/L Mn. Accuracy of the analytical method was evaluated by comparing the expected metal concentrations in certified reference materials with the measured values. Simultaneous performance of analytical blanks, standard reference (JG-3) (Imai *et al.*, 1995) and calculation of the average recoveries of heavy metals confirmed that the accuracy of the method was within acceptable limits (Table 1).

DISCUSSION

The Soltan Meydan Basaltic Formation area is located at front of structural regime, Eastern Alborz Mountains, and represents a great deal of thrusts, strike-slip faults and distinct topographic changes particularly along the borderline between the mountain and the plain. The amount of S_{mf} index (Eq. 1) which indicates the intensity of tectonic activity, along a section with 12 Km in length (L-L´) was calculated to be 1.2 represents a region with high structural activity (Wells *et al.*, 1998; Malik and Mohanty, 2007). Generally, the mountain front curving pattern, formed fractures and faults, and geologic features such as triangular facets, V-shaped valleys, alluvial canals and stream systems all confirm that the area is tectonically intensely active. According to the Photo-lineament Factor (PF) value of the study area which demonstrates high-fractured areas (Fig. 3), it can be understood that there is a connection between fractures and development of the stream-drainage system. On the other hand, a high frequency of fractures on the mountain front provides favorable conditions in terms of developing the drainage system. Most of the streams follow a general structural trend which indicates that these drainages may be structurally controlled. Less-developed branches of streams could be regarded as an indicator of crushed zones at which sediments are accumulated in the bigger branches (Duk-Rodkin *et al.*, 2003). In the study area streams show a complex pattern depending on the fractures, additionally, in many cases the relationship with different classes of faults whether they are major or minor is observable.

As a result of weathering, streams disperse elements through water and finally, deposit them as sediments, so high-concentrated stream sediment samples may reveal potentially mineralized areas. The chemical composition of 7 target elements of stream sediments from different parts of the study area has been shown in table 1. The result of the geochemical analysis shows that the average values of Cu (33-106.54 ppm) and Zn (40.88-376 ppm) in the area are 69.29 and 165.61 ppm respectively, but In the A1 area samples (including S4 through S11) it is 88.2 ppm for Cu and 291.62 ppm for Zn. In the A2 area samples (including S56 through S61) the average value is 91.52 ppm for Cu and 204.76 ppm for Zn. The average value of Pb (14.46-189.04 ppm) and Co (8.2-88.64 ppm) among all the samples is indicated 62.42 ppm and 36.51 ppm respectively, which changes to 136.41 and 75.18 ppm in the A1 area samples. The average concentration for Ni (15.14-73.24 ppm), Mn (321.6-1326.4 ppm) and Fe (2.28-5.39 wt%) is 50.66 ppm, 713.08 ppm and 3.72 wt% respectively, which increases to 61.81 ppm, 1073.61 ppm and 5.07 wt% as the average values of Ni, Mn and Fe in the A2. Briefly, the A1 and A2 areas show, in turn, high quantity of Cu-Zn-Pb-Co and Cu-Zn-Ni-Mn-Fe elements. As it is shown on figure 3, these areas follow the high-fractured areas which are explained with high-PF values and may be related to the possible mineralization.

CONCLUSION

(1) In this study, it has been suggested that by using stream sediment exploration technique, it is possible to identify regional anomalies, which are useful in defining areas for exploration.

(2) Distribution pattern of Cu, Pb, Zn, Ni, Co, Mn and Fe in sediments of the study area is useful to indicate those mineral potential areas where new mineral deposits may exist.

(3) It is suggested that there is a close relationship between Photo-lineament Factor (PF) value, showing high-fractured areas, and enrichments of Cu, Pb, Zn, Ni, Co, Mn and Fe elements, which can be regarded as an exploratory tool. It is suggested that bedrock chemistry, mobility of elements, dispersion mechanism, climate, nature of weathering, pH of the dispersing water and distance from the mineralized bedrock might has played an important role in the distribution of these elements in the stream sediments.

Funding: This study received no specific financial support.

Competing Interests: The authors declare that they have no competing interests.

Contributors/Acknowledgement: All authors contributed equally to the conception and design of the study. B. Shafiei (Golestan University) and M. A. Rajabzadeh (Shiraz University) are gratefully acknowledged who kindly provided helpful comments and suggestions during this study. The authors would like also to thank the Editor-in-Chief, Editorial Board and reviewers of the journal for editorial handling.

REFERENCES

Alavi, M., 1996. Tectonostratigraphic synthesis and structural style of alborz mountain system in northern iran. Journal of Geodynamics 21: 1-33.

Atsuyuki, O., I. Noboru, T. Shigeru and T. Yoshiko, 2005. Influence of surface geology and mineral deposits on the spatial distributions of element concentrations in the stream sediments of hokkaido japan. Journal of Geochemical Exploration 86: 86-103.

Berberian, M., 1983. The southern caspian: A compressional depression floored by a trapped, modified oceanic crust. Canadian Journal of Earth Sciences 20: 163-183.

Bishop, M.P., 2001. Topographic analysis and modeling for alpine glacier mapping. Polar Geography 25: 182-201.

Bull, W.B. and L.D. McFadden, 1977. Tectonic geomorphology north and south of the garlock fault. California: Proceedings of the Eighth Annual Geomorphology Symposium.

Bull, W.L., 1997. Discontinuous ephemeral streams. Geomorphology 19: 227-276.

Champan, R.G., R.C. Leake, D.P.G. Bond, V. Stedra and B. Fairgrieve, 2009. Chemical and mineralogical signatures of gold formed in oxidizing chloride hydrothermal systems and their significance within populations of placer gold grains collected during reconnaissance. Economic Geology 104: 563-585.

Dugmore, M.A., L.P. W. and R. Philip, 1996. Discovery of the mt. Bini porphyry copper-gold-molybdenum deposit in the owen stanley ranges, papua new guinea-a geochemical case history. Journal of Geochemical Exploration 57: 89-100.

Duk-Rodkin, A., R.A. Chan and K.G. McQueen, 2003. Drainage evolution and implications for neotectonics and mineral exploration in the cobar uplands, nsw. CRC LEME Regional Regolith Symposia 104-109.

Duncan, C.C., 1998. Comparison of late pleistocene and modern glacier extents in central nepal based on digital elevation data and satellite imagery. Quaternary Research 49(241-254).

Ghavidel-Syooki, M., 2000. Biostratigraphy and palaeogeography of late ordovician and early silurian chitinozoans from the zagros basin, southern iran. Historical Biology 15: 29-39.

Ghavidel-Syooki, M. and M. Vecoli, 2007. Latest ordovician-early silurian chitinozoans from the eastern alborz mountain range, kopet-dagh region, northeastern iran: Biostratigraphy and palaeobiogeography. Review of Palaeobotany and Palynology 145: 173-192.

Hardcastle, K.C., 1995. Photo-lineament factor: A new computer-aided method for remotely sensing the degree to which bedrock is fractured. Photogrammetric Engineering and Remote Sensing 61: 739-747.

Honarmand, M. and M. Ranjbar, 2004. Application of different image processing techniques on etm+ images for exploration of porphyry and vein type copper mineralizations in kuh-e-mamzar and kuh-e-panj areas, kerman province. Geosciences 57: 110-127.

Imai, N., S. Terashina, S. Itoh and A. Ando, 1995. Compilation of analytical data for minor and trace elements in seventeen gsj geochemical reference samples, igneous rock series. Geostandard Newsletter 19: 135-213.

Le Couteur, P.C. and J.A. Mcleod, 2006. Heavy mineral processing at vancouver indicator processors inc./teck cominco global discovery lab. Newsletter of the Association of Applied Geochemists 133: 15-18.

Malik, J.N. and C. Mohanty, 2007. Active tectonic influence on the evolution of drainage and iandscape: Geomorphic signatures from frontal and hinterland areas along the northwestern himalaya, india. Journal of Earth Sciences 29: 604-618.

Masoud, A. and K. Koike, 2006. Tectonic architecture through landsat-7 etm+/ srtm dem-derived lineaments and relationship to the hydrogeologic setting in siwa region, nw egypt. Journal of African Earth Sciences 45: 467-477.

Mehdizadeh, S., H., 2008. Pre-rifting evidence of paleotethys in the southwest of shahrood, northeastern iran. World Applied Sciences Journal 3: 54-161.

Ohta, A., N. Imai, S. Terashima and Y. Tachibana, 2004. Investigation of elemental behaviors in chugoku region of japan based on geochemical map utilizing stream sediments. Geochemistry 38: 203-222.

Paul, F., C. Huggel and A. Kääb, 2004. Combining satellite multispectral image data and a digital elevation model for mapping debris-covered glaciers. Remote Sensing of Environment 89(4): 510-518.

Sarala, P. and V. Peuraniemi, 2007. Exploration using till geochemistry and heavy minerals in the ribbed moraine area of southern finnish lapland. Geochemistry: Exploration, Environment, Analysis 7: 195-205.

Sekabira, K., H. Oryem-Origa, T.A. Basamba, G. Mutumba and E. Kakudidi, 2010. Assessment of heavy metal pollution in the urban stream sediments and its tributaries. International Journal of Environment, Sciences and Technology 7(3): 435-446.

Seleem, T.M., 2013. Analysis and tectonic implication of dem-derived structural lineaments, sinai peninsula, egypt. International Journal of Geosciences 4: 183-201.

Singh, M., 2003. Geogenic distribution and baseline concentration of heavy minerals in sediments of the ganges river, india. Journal of Geochemical Exploration 80: 1-17.

Solomon, S. and Gh. Ghebreab, 2006. Lineament characterization and their tectonic significance using landsat tm data and field studies in the central highlands of eri- trea. Journal of African Earth Sciences 46: 371-378.

Wells, S.G., T.F. Bullard, C.M. Menges, P.G. Drake, P.A. Karas, K.I. Kelson, J.B. Ritter and J.R. Wesling, 1998. Regional variations in tectonic geomorphology along a segmented convergent plate boundary, pacific coast of costa rica. Geomorphology 1: 239-266.

Figure 1: A) Location of the Soltan Meydan Basaltic Formation area in Northern Iran, B) Satellite image of the area, C) Simplified geological map of the area.

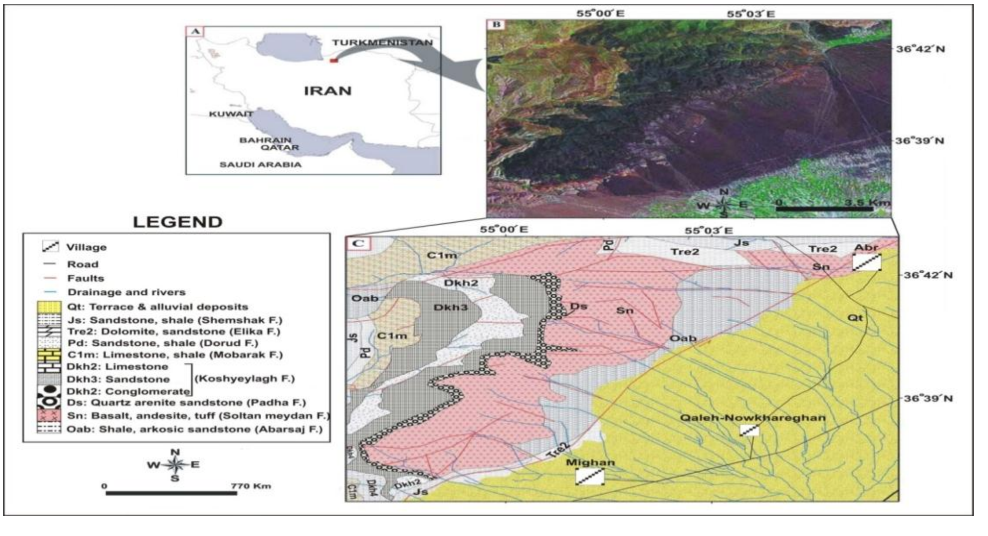

Figure 2: A 3D map of the Soltan Meydan Basaltic Formation area; A) A view of Abr village along with mechanism of Northern Shahrud fault, B) Location of 50-meter shift in Quaternary alluviums.

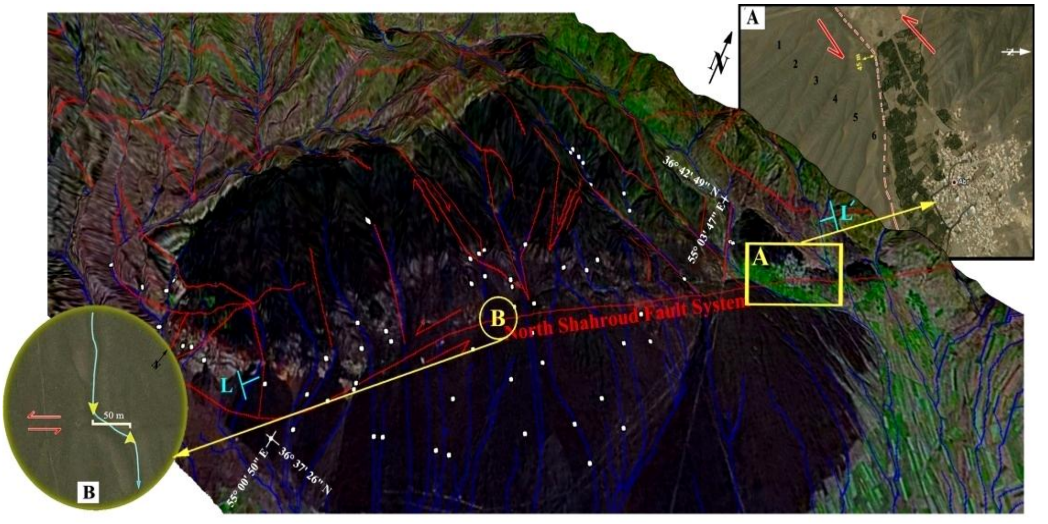

Figure 3: Distribution contour map of Photo-lineament Factor (PF) index value.

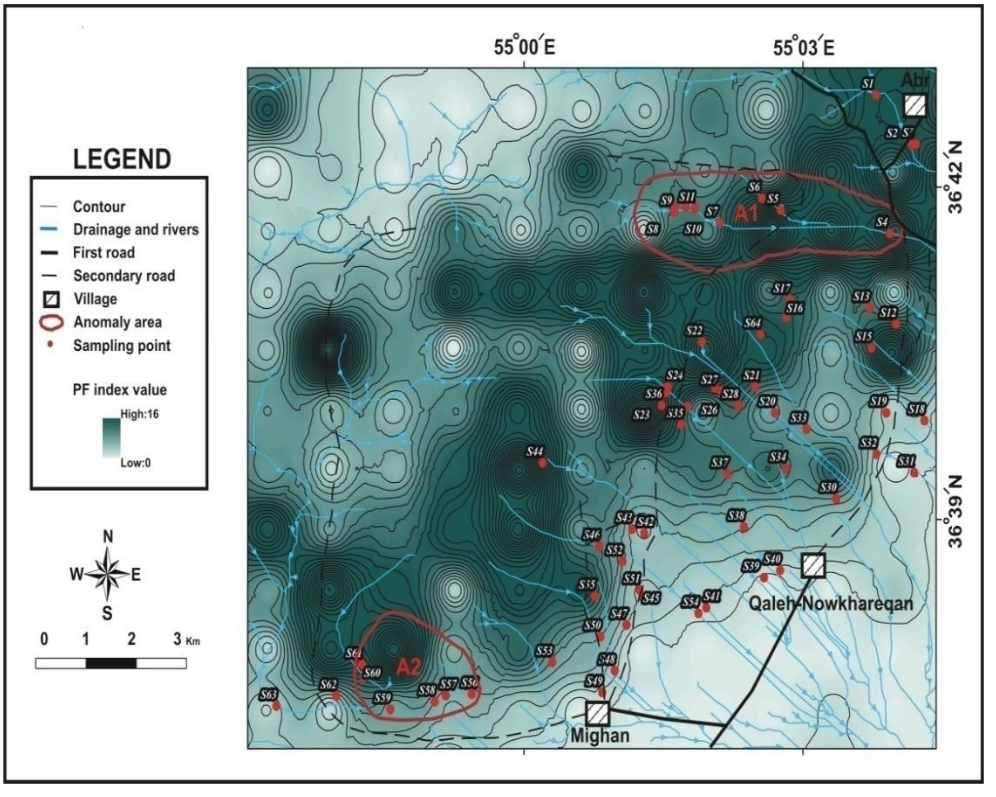

Figure 4: Location of sampling points and streams in the Soltan Meydan Basaltic Formation area.

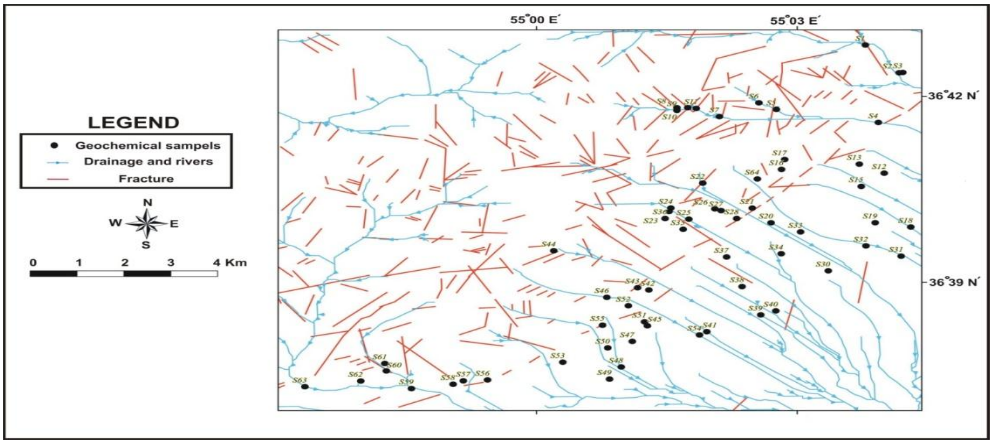

Table 1: Chemical composition of 7 target elements from AAS-analyzed stream sediments (in ppm except Fe in wt%).

Sample	S1	S2	S3	S4	S5	S6	S7	S8	S9	S10	S11	S12	S13	S15	S16	S17
Cu	56.47	51.09	61.46	77.99	85.31	91.81	81.07	83.44	98.86	92.21	94.91	54.39	61.18	65.86	67.59	77.22
Pb	41.8	43.74	59.02	107.6	119.78	102.3	147.32	189.04	166.2	124.9	134.18	51.48	70.1	70.92	70.44	95.14
Zn	127.39	125.29	202.46	272.5	237	235.5	311.9	376	311.05	290.8	298.23	161.9	156.17	169.95	183.31	208.9
Ni	43.04	48.64	54.42	43.66	53.18	50.92	38.64	41.54	56.28	38.14	30.78	50.4	59.4	69.24	61.42	63.24
Co	26.68	21.62	42.84	73.86	67.7	69.6	81.04	80.64	88.64	71.3	68.72	35.84	31.52	33.46	42.5	45.44
Mn	727.4	696.4	930.4	977.9	842.6	800.9	606.7	726.4	853.2	505.8	759.7	813.3	959.5	733.2	827.2	793.9
Fe	3.76	3.34	4.3	3.62	3.95	2.95	2.66	3.62	3.95	2.95	2.66	3.87	3.97	3.61	3.85	3.99

Sample	S18	S19	S20	S21	S22	S23	S24	S25	S26	S27	S28	S30	S31	S32	S33	S34
Cu	55.86	57.54	58.54	56.4	78.15	67.93	69.41	98.74	71.97	59.43	55.29	74.71	66.47	68.23	45.45	57.93
Pb	63.64	55.52	35.08	64.04	92.08	71.68	50.22	51.4	74.3	54.76	49.14	69.1	60.66	60.32	44.34	33.98
Zn	157.5	164.37	111.9	130.3	205.8	158.3	142.5	121.9	151.2	122.4	106.8	158.0	157.06	168.22	136.19	98.6
Ni	57.96	61.2	33.12	54.6	72.58	60.26	46.26	49.98	58.18	50	47.02	50.98	52.96	64.46	39.6	33.26
Co	34.44	42.7	28.96	28.9	58.4	26.9	40.52	37.5	24.18	25	25.36	35.94	43.52	39.1	33.58	30
Mn	689.2	773.5	466.6	894.2	877.9	763	863.9	695.8	840.7	623	533.3	690.6	702.1	827.6	578.7	457.8
Fe	4	4.02	2.93	3.99	4.35	2.86	4.36	3.93	3.15	3.36	3.01	3.73	3.89	3.98	3.66	2.92

Sample	S35	S36	S37	S38	S39	S40	S41	S42	S43	S44	S45	S46	S47	S48	S49	S50
Cu	63.16	79.73	72.32	61.22	78.52	57.71	59	58.75	67.02	61.53	61.11	79.7	56.4	65.51	52.64	62.24
Pb	70.04	64.36	56.42	52.88	46.36	56.86	60.44	62.26	73.58	34.34	39.82	40.12	55.04	42.26	46	57.8
Zn	177.07	140.41	122.52	113.57	114.59	160.78	186.67	191.5	197.2	87.69	81.19	126.5	163.7	115.4	149.45	187.81
Ni	65.88	62.52	52.3	49.9	50.8	58.36	56.24	60.82	47.26	44.26	42.82	42.3	60.18	41.62	61.98	49.86
Co	41	23.62	33.06	31.52	32.5	36.32	46.58	41.54	34.36	24.72	20.44	29.44	36.52	31.08	31.96	37.72
Mn	809.9	796	636.7	572.1	603.7	731.8	824.5	749.6	667.3	479.8	474.6	514.7	641.4	494.5	637.8	645.6
Fe	4.04	3.14	4.15	3.67	3.84	4	4.66	4.1	3.39	3.42	3.1	3.85	3.91	4	3.62	3.95

Sample	S51	S52	S53	S54	S55	S56	S57	S58	S59	S60	S61	S62	S63	S64
Cu	71.62	58.72	63.93	83.16	73.79	89.33	106.54	90.69	91.03	86.28	85.28	36.57	33	47.11
Pb	30.36	34.74	56.86	48.04	36	45.92	46.82	27.2	24.76	14.70	14.46	28.24	39.46	40.24
Zn	74.86	84.9	183.32	82.34	70.11	202.72	234.61	281.04	253	123.61	133.62	40.88	88.17	139.34
Ni	40.8	40.44	59.04	36.16	35.6	63.18	65.34	73.24	68	51.07	50.06	15.14	28.1	32.58
Co	20.06	18.44	51.38	20.9	17.06	27.92	28.06	26.28	8.2	8.58	8.28	11.12	10.18	38.94
Mn	453.9	389.2	698.7	408.9	451.3	1233.2	1080.9	1006.7	1326.4	897.9	896.6	324.1	321.6	609.6
Fe	2.95	2.66	4.54	3.22	3.03	5.32	5.31	5.34	5.39	4.51	4.58	2.28	2.3	3.67